

Strain Induced Modifications of Optoelectronic Properties of PbSe Nanostructures

M. Simma, D. Lugovyy, T. Fromherz, G. Springholz, G. Bauer

Institut für Halbleiter- und Festkörperphysik,
Universität Linz, A-4040 Linz, Austria

Deformation potentials D_u and D_d for PbSe were analyzed using transmission data of PbSe/PbEuSeTe multi-quantum wells. We use calculations based on a kp model to obtain the strain induced intervalley splitting in the quantum wells. For the reduction of the Fabry-Pérot interference fringes of the multilayer structures 480 Å NiCr anti-reflex coating is deposited on top of the multi-quantum wells. At low temperature we found PbSe deformation potentials $D_u = -1.97$ and $D_d = 5.88$. The results of the transmission measurements are compared with photo-current spectra measured with self-assembled PbSe/PbEuTe quantum dot superlattices.

Introduction

For the design of heterostructure optoelectronic devices the accurate knowledge of deformation potentials is of crucial importance. In the narrow gap IV-VI semiconductors due to large deformation potentials, even moderate strain values result in significant shift of the band edges. Theoretically [3], [2] and experimentally [8], [5] determined deformation potentials are spread over a wide range, especially the biaxial deformation potentials components. For example, according to Zaslavskii et al. [8] the uniaxial deformation potential component for PbSe D_u varies from -0.2 to -3.7 eV. In addition, most values do not agree with the isotropic deformation potentials, which can be measured with high accuracy from hydrostatic pressure experiments.

Experimental

IV-VI semiconductors are soft materials and therefore, it is rather difficult to produce uniaxial strains by applied external forces. In this work, the strain in PbSe layers result from the lattice mismatch between the constituting materials of epitaxial PbSe/PbEuSeTe multi-quantum well structures (MQW). The heterostructures are grown on (111) oriented BaF₂ substrates in a molecular-beam epitaxy (MBE) system. The 80 periods MQWs were grown on 1.5 μm fully relaxed buffer layers consisting of PbEuSeTe with the same composition as the barrier layers. The strain in the PbSe QWs is caused by the lattice mismatch to the PbEuSeTe buffer and barrier layers. The latter is determined mainly by the Te content in the quaternary layers, for which the lattice constant follows the same Vegard's law as for PbSeTe. Thus, for the used quaternary composition of $y_{Te} = 6 - 14\%$ the strain in the PbSe QWs varies between $\epsilon_{||} = 0.48 - 1.1\%$. The barrier height, on the other hand, is mainly determined by the Eu concentration due to the very large bandgap increase with increasing Eu content. For $x_{Eu} \approx 8\%$ used in this work, the energy band gap of the PbEuSeTe barrier layer is about 290 meV larger than that of PbSe. The thin PbSe 40 Å quantum wells (QW) are grown below the critical layer thickness and are pseudomorphically strained. Using this material

system we have the possibility to tune the energy gap in the barriers and the strain in the QWs virtually independently by the Eu and Te content of the PbEuSeTe alloy.

Samples with different strain values and similar Eu content were investigated using Fourier transform infrared spectroscopy (FTIR). Transmission spectra of the PbSe/PbEuSeTe MQWs were measured at temperatures between 6 K and 300 K in the spectral range of 500 cm^{-1} to 6000 cm^{-1} with a resolution of 8 cm^{-1} using a Bruker IFS-113v Fourier transform spectrometer.

Using two spectra measured at slightly different temperatures, we obtain the differential transmission as the logarithm of the ratio between the spectra measured at higher temperature and lower temperature. This approach takes advantage of the very strong temperature dependence of the PbSe and PbEuSeTe bandgaps and consequently, of the energy levels in the QWs, which results in pronounced peaks in the differential transmission spectra at the transition energies. Additionally, the differential spectra show much less pronounced Fabry-Pérot interference fringes caused by the layer refractive index contrast between the transparent BaF_2 substrate ($n \approx 1.5$) and the IV-VI epilayers ($n \approx 4.5$). This is due to the fact that the dielectric constants of the materials in the multilayer structure vary only weakly with temperature. For further reduction of the Fabry-Pérot interference fringes 480 \AA NiCr [11] anti-reflection coating was deposited on the multilayer stack of the samples.

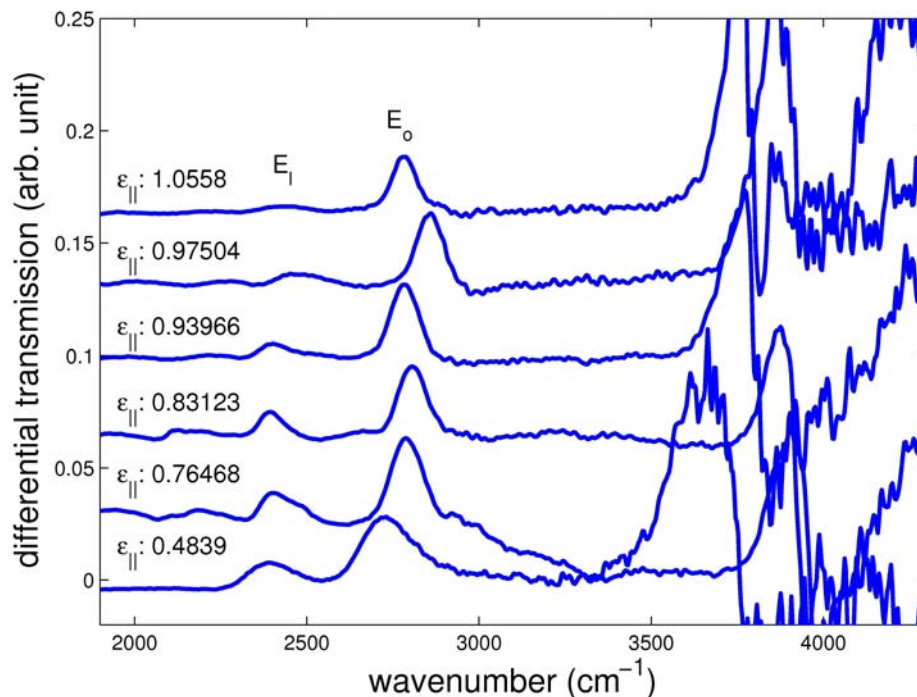


Fig 1: Differential transmission spectra of PbSe/PbEuSeTe MQWs for different strain values. As the strain increases, the L-valley splitting between the longitudinal (E_I) and the oblique valley (E_o) increases.

For each sample, the differential transmission shown in Fig. 1 exhibits three peaks caused by the optical transitions related to the longitudinal (E_I) and oblique L-valleys (E_o) in the PbSe QWs and the PbEuSeTe fundamental absorption in the barrier layers. Because of the narrow 40 \AA PbSe well width no transitions to higher energy levels can be observed, indicating that higher energy levels are not confined in the QWs. The peaks related to the longitudinal valley transition show a weaker intensity compared to the peaks of the oblique valleys. This is due to the threefold degeneracy of the oblique

valleys. The clearly resolvable L-valley splitting Δ (see Fig. 1) increases with increasing strain. This intervalley splitting is caused on the one hand by the different effective electron and hole masses along the confinement direction of the oblique and longitudinal valleys, on the other hand by the different band gap shifts due to the biaxial strain in the layers. In thick epitaxial layers where the confinement shift of the optical transitions is zero the intervalley splitting is equal [8]

$$\Delta = \delta E_g^N - \delta E_g^O = \frac{8}{9} D_u (\varepsilon_{\perp} - \varepsilon_{\parallel}) \quad (1),$$

where D_u denotes the uniaxial component of the deformation potentials and ε_{\parallel} and ε_{\perp} are the in-plane and perpendicular strains, respectively. In smaller QWs the optical transition energies as well as the intervalley splitting is increased by the quantum confinement effect. Therefore, in order to be able to apply Eq. 1 the confinement energies have to be subtracted from the measured transition energies.

The energy levels in the PbSe quantum wells can be calculated numerically with high accuracy using the envelope function method based on a kp model if the confinement energies in valence and conduction band are known. We estimated these confinement energies assuming that the unstrained PbSe/PbEuSeTe band-offsets in valence and conduction bands are equal ($\Delta E_c = \Delta E_v$), due to the mirror like bandstructure [7] of these materials. For the calculation of ΔE_v we used temperature dependent energy gaps of PbEuSe and PbEuTe given in [9] and [10], where the energy gap of PbEuSeTe is linearly interpolated.

The influence of the strain on the band-edge energies is given by the expression

$$\delta E = \sum D_{ij}^{c,v} \varepsilon_{ij} \quad (2),$$

where $D_{ij}^{c,v}$ is the deformation potential tensor in the conduction and valence band and ε_{ij} denotes the strain tensor. In cubic systems this expression is simplified to two components $D_u^{c,v}$ and $D_d^{c,v}$ i.e., the uniaxial and dilatation deformation potentials and the ε_{\perp} and ε_{\parallel} strain components.

The change in the bandgap is then characterized by the deformation potentials D_u and D_d which are equal to the difference of the $D_u^{c,v}$, $D_d^{c,v}$ values of the conduction and valence bands. Using deformation potentials given in literature [3] we calculated from the optically measured transition energies the strain induced intervalley splitting. To derive the uniaxial deformation potential constant D_u with the help of Eq. (1) the calculated energy levels are subtracted from the measured transition data. For the 6 K measurement we get for D_u a value of -1.97 eV and at 77 K a value of $D_u = -2.39$ eV. Using the relation $D_{iso} = 3D_d + D_u$ and $D_{iso} = 15.7$ eV for the isotropic deformation potential constants [5] we calculated the dilatation deformation potential as $D_d = 5.88$ eV and $D_d = 6.03$ eV at 6 K and 77 K, respectively. The measured values for D_u agrees well with the theoretically determined values given in [3], [2].

Assuming a symmetric band offset in the unstrained case and the theoretical deformation potentials values given in Ref. [3], one obtains a rapidly increasing band offset asymmetry with increasing strain in the PbSe layers. In particular a type I - type II band alignment discontinuity transition is expected at strain values larger than about 80% for the given Eu concentration of 8%. Thus, at high strain values the PbSe valence band edge lies energetically below the barrier valence band edge. In this case, the PbSe valence band acts as barrier for the holes. For such a type II band alignment, the spatially indirect optical transitions are much weaker due to the reduced wavefunction overlap. The upper spectra in Fig. 1 resulting from the highly strained MQW structures exhibits a significantly weaker longitudinal valley peak than the spectra of the other samples.

Indications for such a type II band alignment are also obtained from photo-current (PC) measurements on highly strained PbSe/PbEuTe self-assembled quantum dot superlattices. These superlattices were grown by MBE onto (111) BaF₂ substrates [4] on 1.5 μm PbEuTe buffer layers at 340 – 420 °C. On these buffer 5 – 8 monolayers of PbSe were grown followed by a PbEuTe spacer layer with 6% Eu content and a thickness varying between 250 and 650 Å. The strain in the thin epitaxial PbSe layer resulting from the lattice misfit between PbSe and PbEuTe relaxes via island formation. This island formation starts after deposition of 3 ML PbSe [4] which compose a 2D wetting layer. By deposition of many PbSe/PbEuTe bilayers, a highly efficient 3D dot ordering takes place [4]. Using FTIR spectroscopy, we performed spectral resolved lateral photo-current measurements on these self-assembled QD structures.

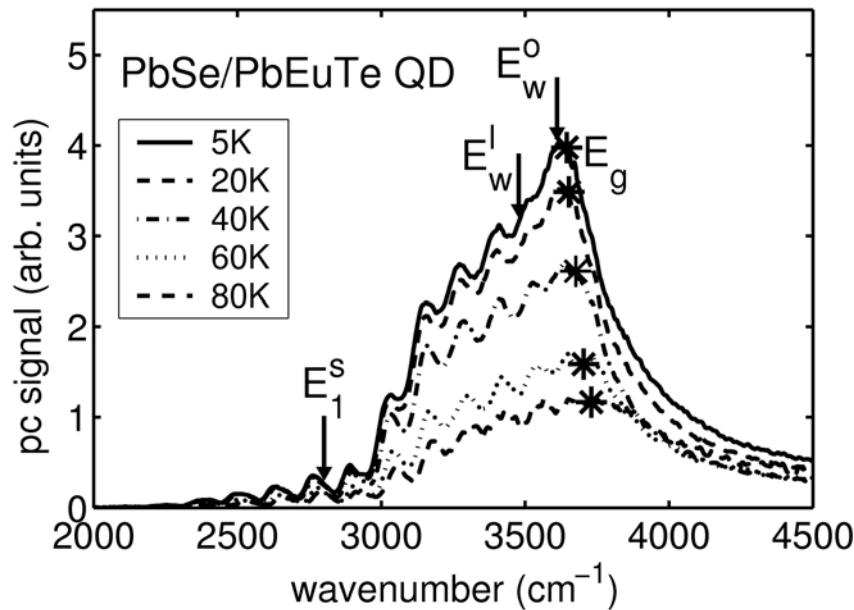


Fig 2: Photo-response of a PbSe/PbEuSeTe QD superlattice for different temperatures. Arrows indicates the optical transitions to different structures in the superlattice: E_1^s PbSe QD, E_w^l and E_w^o longitudinal and oblique wetting layer valley. The barrier bandgap E_g is marked with (*).

For a type I band alignment one would expect a freeze out of the carriers in the QD at low temperature resulting in vanishing lateral pc-signal. Figure 2 shows the photo-response measured at different temperatures performed with 50 Å high QD. The transition energies caused by various structures in the QD structures are marked by arrows. The arrow labeled as E_1^s is related to the QD ground s-state transition. The arrows labeled by E_w^l and E_w^o are the ground state transitions of the longitudinal and oblique valleys in the wetting layer. The quantum size energies in the dots and the wetting layer were calculated with the envelope function method using a kp model. For the QDs a simplified spherical shape [1] was assumed. The absorption edge at 3800 cm⁻¹ marked by * is caused by the buffer and barrier layer fundamental transition. Clearly the pc-signal is well resolved for all temperatures, in particular, no freeze out of the carriers is observed. This indicates a type II band alignment of the PbSe QD. Assuming a band discontinuity of 120 meV between the PbSe/PbTe valence band edges [6] leads to a type I band alignment in the unstrained case. Using deformation potentials given in [3] shifts the valence band edge of PbSe below the PbEuTe valence band edge. This

assumptions result in a type II band alignment which explains the observed pc-signal at low temperatures.

Conclusion

In summary, strained PbSe multi-quantum wells and quantum dot superlattices structures were investigated by FTIR spectroscopy. We deposit a NiCr anti-reflection coating on the MQW samples in order to reduce the Fabry-Pérot interference fringes. Longitudinal and oblique valley subband transitions were observed and from the intervalley splitting the PbSe deformation potentials were determined. For increasing strain in the samples we observe a transition from type I to type II band alignment. Temperature dependent spectrally resolved photo-response of PbSe QD superlattices does not show any freeze out of the carriers. This indicates a type II band alignment of the PbSe dots.

Acknowledgments

Work supported by Öster. FWF Forschung, SFB IRON, Projekt Nr. F2504-N08.

References

- [1] M. Califano and P. Harrison: *J. Appl. Phys.*, 86, 5054, (1999).
- [2] P. Enders: *Phys. Status Solidi B*, 129, 89, (1982); 132, 165, (1985).
- [3] L. G. Ferreira: *Phys. Rev.*, 137, 1601, (1965).
- [4] G. Springholz, V. Holy, M. Pinczolit, and G. Bauer: *Science*, 282, 734, (1998).
- [5] M. V. Valeiko, I. I. Zasavitskii, A. V. Marveenko, B. N. Matsonashvili, and Z. A. Rukhadze: *Superlattices. Microstruct.*, 9, 195, (1991).
- [6] S. H. Wei and A. Zunger: *Phys. Rev B*, 55, 13605, (1997).
- [7] G. Bauer: *Narrow Gap Semiconductors: Physics and Applications*, Vol. 133, Springer Lecture Notes in Phys., edited by W. Zawadski (Springer, Berlin, 1980), p. 427.
- [8] I. I. Zasavitskii, E. A. de Andrada e Silva, E. Abramof, and P. J. McCann: *Phys. Rev. B*, 70, 115302–1, (2004).
- [9] T. Maurice, F. Mahoukou, G. Breton, S. Charat, P. Masri, M. Averous, and R. Bisaro: *Phys. Stat. Sol.*, (b) 209, 523, (1998).
- [10] S. Yuan, H. Krenn, G. Springholz, and G. Bauer: *Phys. Rev. B*, 47, 7213, (1993).
- [11] S. W. McKnight, K. P. Stewart, H. D. Drew, and K. Moorjani: *Infrared Phys.* 27, 327 (1987)